Application of wall forcing methods in a turbulent channel flow using Incompact3d

S. Khosh Aghdam

Department of Mechanical Engineering - University of Sheffield

Most of large scale engineering flows are turbulent

- Atmosphere
- Transportation (automobile, airplanes, ships,$\cdots$)
- Blood flow in heart

Aim of flow control $\rightarrow$ modify the characteristics of a flow field favourably

- Suppression or enhancement of turbulence
- Dissipation of kinetic energy by turbulent flow around objects
- Increase of resistance to their motion $\rightarrow$ Drag
- Component of the force experienced by a body, parallel to the direction of motion

Enhancement of turbulence

- Mixture in combustion: quality of the fuel-air mixture determines power generation efficiency
- Process industry: quality of mixtures affects chemical reaction rates and purity of final products

Reduction of turbulence

- Drag reduction techniques $\Rightarrow$ energy consumption issues
- Half of the total drag experienced by an aircraft accounts for skin-friction
- Aircraft industry demonstration test: Coverage of fuselage surface with riblet films $\Rightarrow \searrow$ resistance by 2%
- Fuel cost savings (Airbus A320) $\Rightarrow 5 \times 10^4$ L/year $\Leftrightarrow$ saving 200 million $/year

Difficulty in control design ⇒ turbulence → multiscale phenomenon ⇔ coupling of system macroscopic size (L) & Kolmogorov scale (η) by the chaotic process of vortex stretching

- Two main groups ⇒ active and passive
- Categorisation relying on energy expenditure
- Passive ⇒ no energy added in the flow → longitudinal grooves or riblets on a surface
- Active ⇒ input of energy in the flow → blowing and suction jets in opposition control [1]
- Based on the control loops → active techniques categorisation:
  - open-loop (predetermined)
  - closed-loop (interactive)

[1] H. Choi, P. Moin, J. Kim, Active turbulence control for drag reduction in wall-bounded flows, J. Fluid Mech.,262, 75–110, 1994

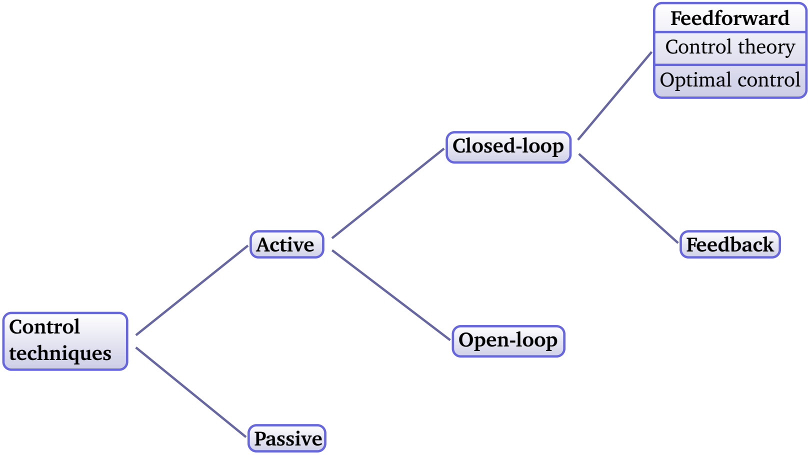
Feedforward
Control theory
Optimal control
Closed-loop
Feedback
Active
Open-loop
Control techniques
Passive

- Skin-friction coefficient

$$C_f = \frac{2\tau_w^*}{\rho^* U_b^2} \tag{1}$$

- Friction velocity

$$u_\tau^* = \sqrt{\frac{\tau_w^*}{\rho^*}} = \sqrt{\nu^* \frac{\partial u^*}{\partial y^*}}\Bigg|_{\text{wall}} \tag{2}$$

- Reduction of velocity gradient ⇒ reduction in drag
- Spanwise wall oscillations (active/open-loop)
- Steady rotating discs [2] (active/open-loop)
- Oscillating rotating discs (active/open-loop)
- Hydrophobic surfaces

[2] Keefe, Method and apparatus for reducing the drag of flows over surfaces - US Patent - 1998

- Applying control to

  Navier-Stokes - continuity equations ⇒ (PDEs)

- PDEs state-space ⇒ infinite-dimensional → $u_x = 0 \Rightarrow$ any $f(y)$ solution ⇒ infinite dimensional solutions space ≠ ODEs state-space → $d\mathbf{y}/dt = 0 \Rightarrow$ solutions in $\mathbb{R}^p$
- Right framework to deal with infinite-dimensional state space solutions ⇒ Functional analysis
- **Functional analysis framework**: functions studied as part of **normed** and **complete** + inner product ⇒ Hilbert
- Why Functional Analysis? ⇒ Banach-L^p spaces too broad for analysing PDEs solution
- **Regularity** properties not always verified in L^p spaces
- **Further assumptions** ⇒ higher order derivatives to ensure regularity (and boundedness) of solutions
- "Higher-order" spaces ⇒ Sobolev → energy spaces

Motivation: design control laws to stabilise a specified equilibrium for the NSE

- NSE $\rightarrow$ nonlinear $\Rightarrow$ nonlinear stability analysis
- Depart from a Lyapunov function $\rightarrow$ energy of the system
- Choose the right norm
- **Example**: function $f(t,x)$ (perturbed variable) with $x \in (0,1)$, within $L^2(0,1) \rightarrow$ prove that:

$$||f(t)||_{L^2(0,1)} \leq C_1 e^{-C_2 t} ||f(0)||_{L^2(0,1)} \quad (3)$$

  $C_1 \geq 1$ overshoot coefficient - $C_2 > 0$ decay rate
- Find conditions for stability $\rightarrow$ not necessarily nonlinear

- **Previous work**: Control law in 2D channel flow → based on wall-tangential actuation (Balogh *et al.* [3]):

$$u(x,y=\pm 1,t) = \mp k \frac{\partial u}{\partial y}(x,\pm 1,t) \tag{4}$$

- Extension to 3D channel flow carried out
- Link the mathematical formulation with a physical problem ⇒ hydrophobic surfaces ⇒ modification of no-slip condition:

$$u = L_s \frac{\partial u}{\partial y}\bigg|_{\text{wall}} \tag{5}$$

- ⇒ Mathematical parameter in [3] ⇔ slip-length
- Relevant scales for MEMS → embedded sensors and actuators in the walls to measure local shear

[3] A. Balogh, W. Liu, M. Krstic, Stability Enhancement by boundary control in 2D channel flow - IEEE Transactions on Automatic Control, Vol.46, No.11 - 2001

- **Objective** ⇒ stabilize a parabolic profile
- Boundary control laws ⇒ decaying kinetic energy w.r.t time ⊗
- Lyapunov-based approach using Lyapunov function:

$$E(\mathbf{w}) = \|\mathbf{w}\|^2_{L^2(\Omega)} = \int_0^{L_z}\int_{-1}^{+1}\int_0^{L_x} (u^2+v^2+w^2)\,\mathrm{d}x\,\mathrm{d}y\,\mathrm{d}z \qquad (6)$$

- ⊗ translates as $\|\mathbf{w}(t)\|_{L^2(\Omega)} \leq C_1 e^{-C_2(t-t_0)}\|\mathbf{w}(t_0)\|_{L^2(\Omega)}$
- Procedure: (**a**) take time derivative of Eq.(6) - (**b**) apply control - (**c**) prove regularity of solutions (involving Sobolev spaces)

L_x	L_y	L_z	Re_p	Δt	time scheme
4π	2.0	$4\pi/3$	4200.0	2.5×10^{-3}	AB2

$L^+ = L \times Re_\tau$	$U^+ = U \times \frac{Re_p}{Re_\tau}$	$T^+ = T \times \frac{Re_\tau^2}{Re_p}$

Parabolic profile, constant mass flow rate, stretched wall-normal

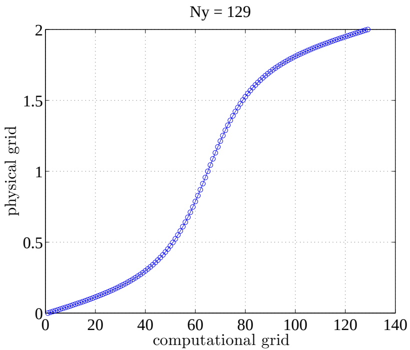

Database of [4] used for comparison at $Re_\tau = 180$

# processors	256	512	1024	2048
runtime (s)	10348	7258	6561	6921

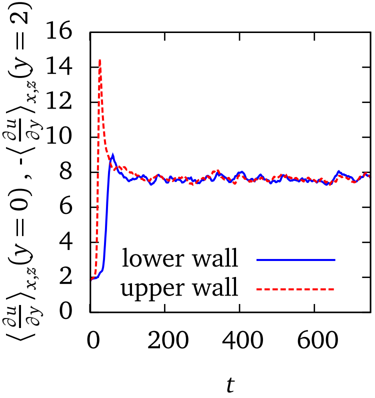

[4] R. Moser, J. Kim, N. Mansour, Direct Numerical Simulations of turbulent channel flow up to $Re_\tau = 590$, Phys. of Fluids, 1999

$\langle \frac{\partial u}{\partial y} \rangle_{x,z}\vert$walls	Re_τ	$C_{f,0}$
7.64	179.1	8.18×10^{-3}

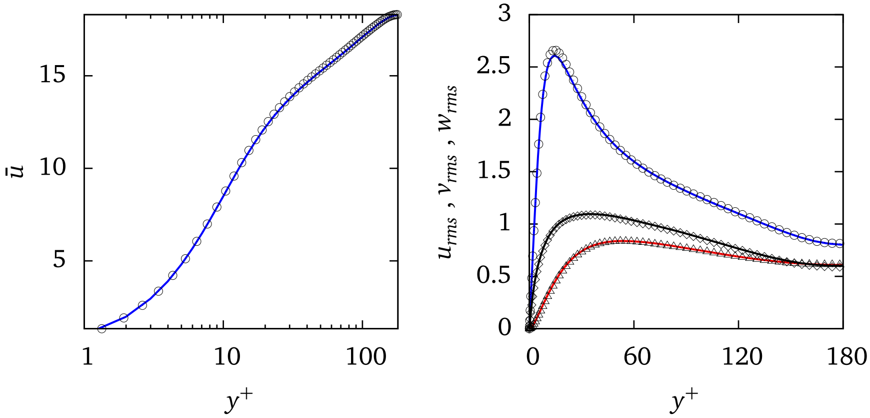

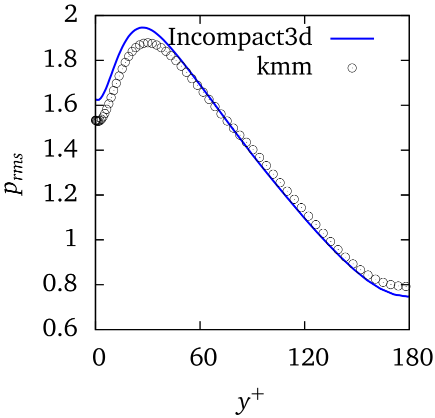
2
1.8
1.6
1.4
1.2
1
0.8
0.6
p_{rms}
Incompact3d
kmm
0
60
120
180
y^+

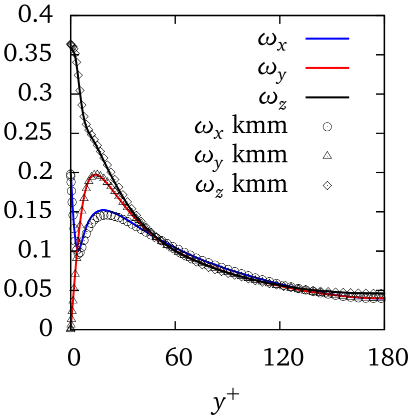
0.4
0.35
0.3
0.25
0.2
0.15
0.1
0.05
0
ω_x
ω_y
ω_z
ω_x kmm
ω_y kmm
ω_z kmm
0
60
120
180
y^+

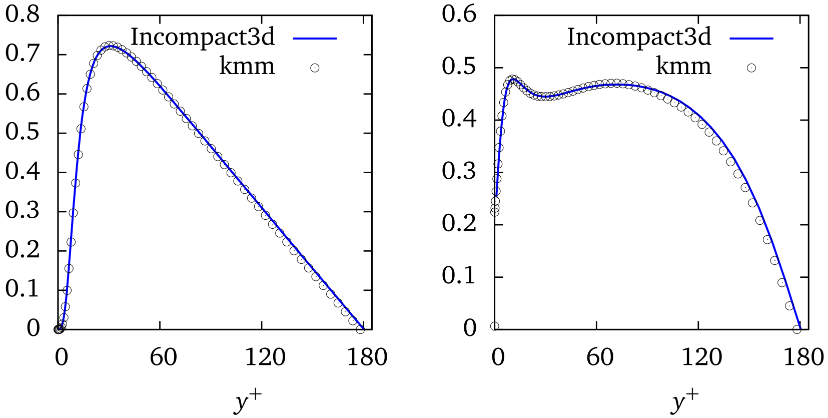

Profiles for $\overline{uv}$ and $\frac{\overline{uv}}{u_{rms}v_{rms}}$

Spanwise wall oscillations: Overview

- DNS of channel flow with this forcing [5] $\Rightarrow$ Drag reduction
- Structure of forcing $\rightarrow w = W_m \sin\left(\frac{2\pi}{T}\right)$
- Dependent on magnitude and period of forcing
- Maximum DR of 40% for $T^+_{\text{opt}} = 100$
- Experimentally [6] found DR $\sim$ 35%

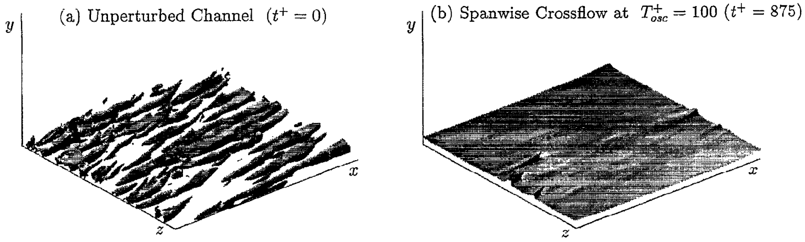

[5] Jung *et. al*, Physics of Fluids, 4, pp 1605–1607 - 1992
[6] Laadhari *et. al*, Physics of Fluids, 6, pp 3218–3220 - 1994

L_x	L_y	L_z	n_x	n_y	n_z	Re_τ	W_m^+	T^+
4π	2.0	$4\pi/3$	256	129	128	200	27.0	125.0

$$DR_{[7]} = 44.5\% \text{ vs } DR_{\text{Incompact3d}} = 44.8\%$$

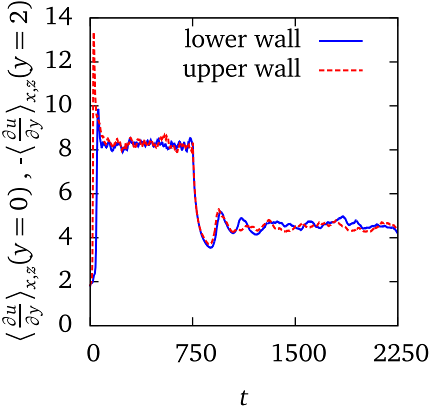

[7] M. Quadrio, P. Ricco, J. Fluid Mech., 521, pp 251–271 - 2004

Vorticity map at the wall

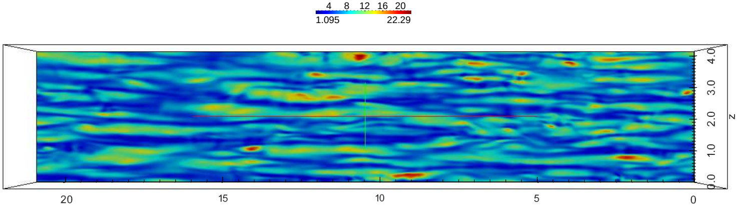

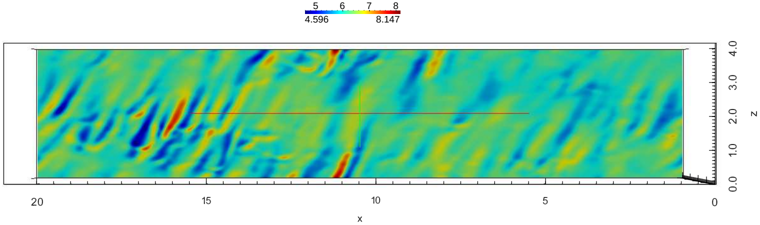

Steady discs rotation: overview

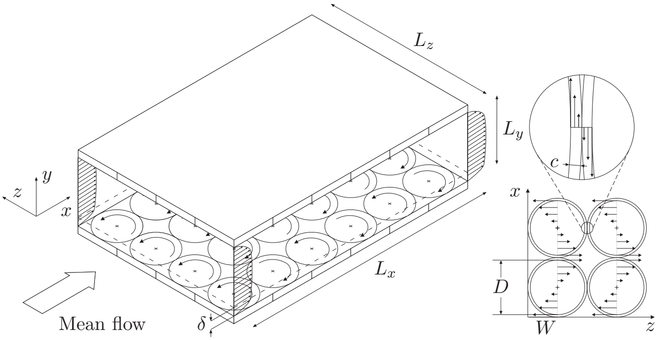

- Active method for DR ⇒ injecting vorticity
- Proposed as part of a patent by Keefe. Numerical study in [8]
- Relevant parameters → (D, W), diameter and maximum tip velocity of the disc

[8] P. Ricco, S. Hahn, J. Fluid Mech., 722, pp 267–290, 2013

Steady discs rotation: implementation

disk_phys.dat
(text file)
from cpp program

→

scr.sh
→ disk_phys_x.dat (text file)
→ disk_phys_z.dat (text file)

→

rfile.f90
→ disk_phys_opacx.dat
(binary direct open-access)
→ disk_phys_opacz.dat
(binary direct open-access)

↓

voir_visu.f90
check process with ParaView
→ tampon_opac_x.vtr
→ tampon_opac_z.vtr
→ tampon_opac_sqr.vtr

←

decomp2d_read_var
interface reads
disk_phys_opacx.dat and
disk_phys_opacz.dat

←

velocity components
distributed on 2D
Cartesian topology
set as boundary conditions

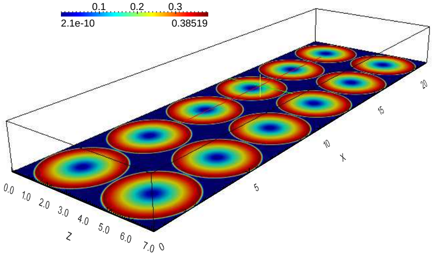

Steady discs rotation: simulations

$L_x \times L_y \times L_z = 6.79\pi \times 2.0 \times 2.26\pi$ - $Re_p = 4200$ - $\mathrm{Nd}_x \times \mathrm{Nd}_z = 6 \times 2$ - $\Delta t = 0.0025$ - $D^+ = 640$ - $W^+ = 9$

KMM $\rightarrow C_f.10^3 = 8.18$

BASE CASE$\rightarrow$ **nx** $\times$ **ny** $\times$ **nz** $= 384 \times 129 \times 256$

$C_{f,0}.10^3$	$C_{f,0}.10^3$	$C_f.10^3$	$C_f.10^3$
Ricco-Hahn	Incompact3d	Ricco-Hahn	Incompact3d
8.25	8.15	6.64	6.62

HIGH RESOLUTION IN $x$$\rightarrow$ **nx** $\times$ **ny** $\times$ **nz** $= 480 \times 129 \times 224$

$C_{f,0}.10^3$	$C_{f,0}.10^3$	$C_f.10^3$	$C_f.10^3$
Ricco-Hahn	Incompact3d	Ricco-Hahn	Incompact3d
8.25	8.13	6.65	6.62

HIGH RESOLUTION IN $z$$\rightarrow$ **nx** $\times$ **ny** $\times$ **nz** $= 384 \times 129 \times 320$

$C_{f,0}.10^3$	$C_{f,0}.10^3$	$C_f.10^3$	$C_f.10^3$
Ricco-Hahn	Incompact3d	Ricco-Hahn	Incompact3d
8.24	8.13	6.63	6.61

HIGH RESOLUTION IN $x,y,z$$\rightarrow$ **nx** $\times$ **ny** $\times$ **nz** $= 512 \times 257 \times 320$

$C_{f,0}.10^3$	$C_{f,0}.10^3$	$C_f.10^3$	$C_f.10^3$
Ricco-Hahn	Incompact3d	Ricco-Hahn	Incompact3d
N/A	8.13	N/A	6.63

Steady discs rotation: flow visualisations

- $\mathbf{u} = \mathbf{u}_\mathrm{m} + \mathbf{u}_d + \mathbf{u}_\mathrm{t} \Rightarrow$ Disc flow: $\mathbf{u}_d = (u_d, v_d, w_d) = \overline{\mathbf{u}} - \mathbf{u}_\mathrm{m}$
- Mean flow: $\mathbf{u}_\mathrm{m}(y) = \langle \overline{\mathbf{u}} \rangle$ with $\overline{\mathbf{f}} \triangleq \frac{1}{t_f - t_i} \int_{t_i}^{t_f} \mathbf{f}\,\mathrm{d}t$ and $\langle \mathbf{f} \rangle \triangleq \frac{1}{L_x L_z} \int_0^{L_z} \int_0^{L_x} \mathbf{f}\,\mathrm{d}x\,\mathrm{d}z$
- Compute 3D $\sqrt{u_d^2 + w_d^2}$ in diagnostic tool + ParaView

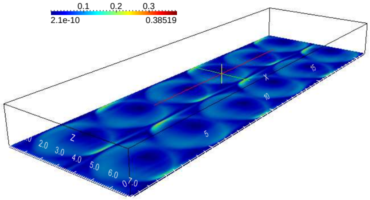

Steady discs rotation: flow visualisations

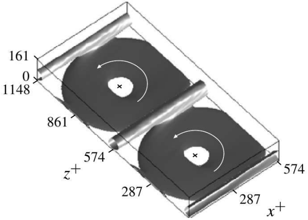

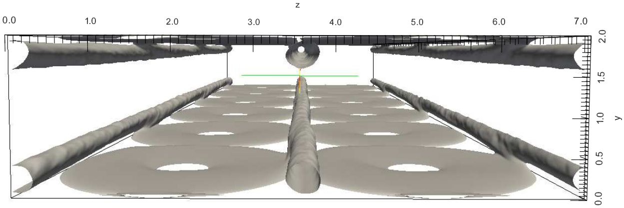

Isosurface representation $\sqrt{u_d^2 + w_d^2} = 0.09$

Steady disccs rotation: flow visualisations

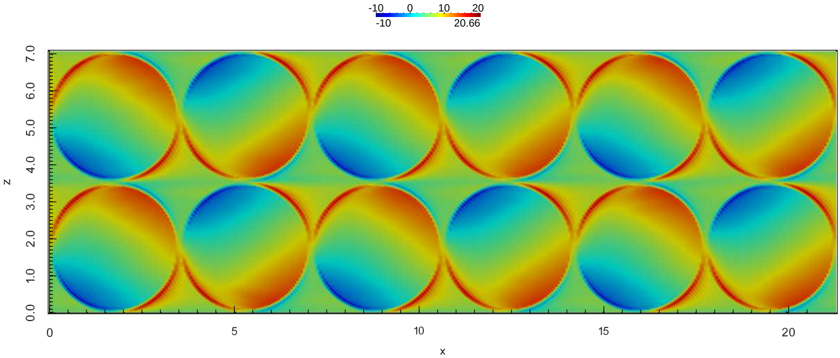

- Time average of the streamwise wall friction $\overline{\frac{\partial u}{\partial y}}\Big|_{y=0}$ in time window $[t_i h/U_P; t_f h/U_P] = [750; 2250]$
- Large regions of negative wall-shear stress

- Rotating discs subject to an oscillatory motion
- Disc tip velocity $\rightarrow W = W_m \cos\left(\frac{2\pi t}{T}\right)$
- Case giving optimal drag reduction

xlx	**yly**	**zlz**	**nx**	**ny**	**nz**	Δt	Re_p
6.79π	2.0	3.39π	384	129	384	2.5×10^{-3}	4200.0

Nd_x	Nd_z	D^+	W^+	T^+
4	2	960	12.0	10^3

Ricco (Conf.)	Incompact3d	Ricco (Conf.)	Incompact3d
$C_{f,0}.10^3$	$C_{f,0}.10^3$	$C_f.10^3$	$C_f.10^3$
8.18	8.13	6.54	6.52

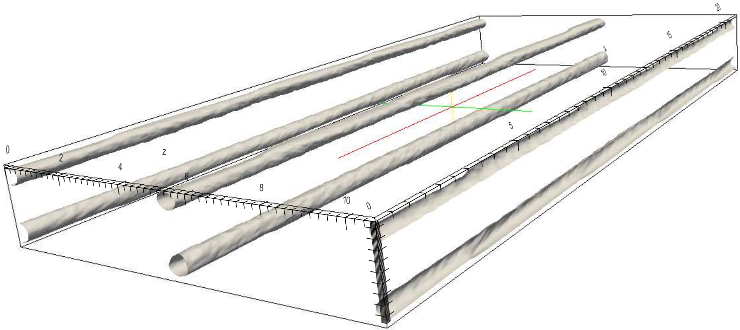

Isosurface representation $\sqrt{u_d^2 + w_d^2} = 0.09$

Hydrophobic surface: finite slip length

- Studied by Min-Kim (2004) with BC forcing term: $u = L_s \frac{\partial u}{\partial y}\Big|_{\text{wall}}$
- u, w and (u, w) can be forced but u gives optimal DR
- $u^{n+1}\Big|_{\text{wall}} = u^n\Big|_{\text{wall}} + L_s \frac{\partial u^n}{\partial y}\Big|_{\text{wall}}$
- Problem: Enforce BC at each time step $\Rightarrow$ Generation of a thin boundary layer [10] $\Rightarrow$ Numerical instability
- Solution in [10] $\rightarrow$ (1) keep the same BC for several time steps - (2) continuous update
- Solution adopted:
  - compute $\frac{\partial u}{\partial y}$ at 1^{st} time step - pass it as BC $\forall t$ ($L_s = 10^{-3}$ (s), $L_s = 2 \times 10^{-3}$ (s) and $L_s = 10^{-2}$ (s))
  - compute $\frac{\partial u}{\partial y}$ at each time step - pass it as BC ($L_s = 10^{-3}$ (s), $L_s = 2 \times 10^{-3}$ (s)and $L_s = 10^{-2}$ (u))

[10] C. Lee, P. Moin, J. Kim, Control of the viscous sulayer for drag redcution, J. Fluid Mech.,14, 2523–2529, 2002

Hydrophobic surface: preliminary results

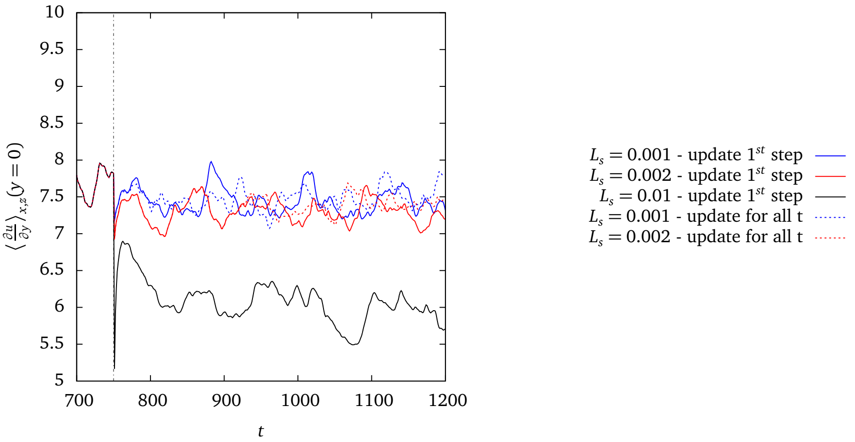

Hydrophobic surface: statistics

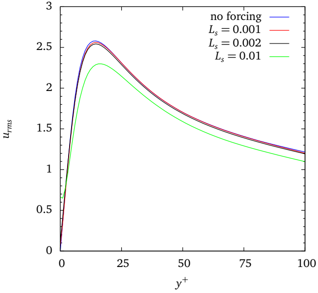

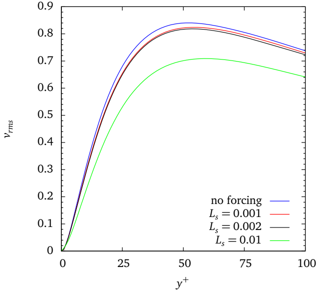

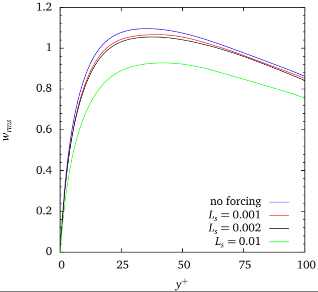

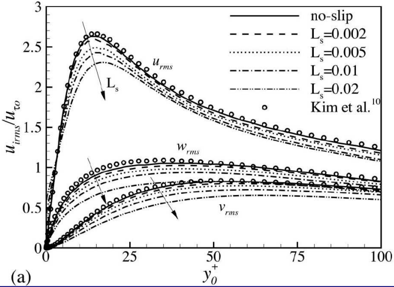

(a)

Hydrophobic surface: Summary

L_s	0.001	0.002	0.01
test_1	updated	updated	crashed
test_2	constant	constant	constant

L_s	$\frac{\partial u}{\partial y}$	DR	DR (Kim-Min 2004)
0.001	updated	2.1%	2%
0.001	constant	2.4%	2%
0.002	updated	4.9%	5%
0.002	constant	4.9%	5%
0.01	updated	NA	18%
0.01	constant	17%	18%

- Incompact3d efficiently dealing with various drag reduction methods
- High scalability allows for future control studies with larger Reynolds number